



HAL
open science

Visualization of Protein Coding, Long Noncoding, and Nuclear RNAs by Fluorescence in Situ Hybridization in Sections of Shoot Apical Meristems and Developing Flowers

Weibing Yang, Christoph Schuster, Nathanaël Prunet, Qingkun Dong, Benoit Landrein, Raymond Wightman, Elliot Meyerowitz

► To cite this version:

Weibing Yang, Christoph Schuster, Nathanaël Prunet, Qingkun Dong, Benoit Landrein, et al.. Visualization of Protein Coding, Long Noncoding, and Nuclear RNAs by Fluorescence in Situ Hybridization in Sections of Shoot Apical Meristems and Developing Flowers. *Plant Physiology*, 2020, 182 (1), pp.147-158. 10.1104/pp.19.00980 . hal-03255550

HAL Id: hal-03255550

<https://hal.inrae.fr/hal-03255550v1>

Submitted on 18 Jan 2022

HAL is a multi-disciplinary open access archive for the deposit and dissemination of scientific research documents, whether they are published or not. The documents may come from teaching and research institutions in France or abroad, or from public or private research centers.

L'archive ouverte pluridisciplinaire **HAL**, est destinée au dépôt et à la diffusion de documents scientifiques de niveau recherche, publiés ou non, émanant des établissements d'enseignement et de recherche français ou étrangers, des laboratoires publics ou privés.



Distributed under a Creative Commons Attribution 4.0 International License

Visualization of Protein Coding, Long Noncoding, and Nuclear RNAs by Fluorescence in Situ Hybridization in Sections of Shoot Apical Meristems and Developing Flowers^{1[OPEN]}

Weibing Yang,^a Christoph Schuster,^a Nathanaël Prunet,^{b,2} Qingkun Dong,^{a,c} Benoit Landrein,^{a,3} Raymond Wightman,^a and Elliot M. Meyerowitz^{a,b,4,5}

^aSainsbury Laboratory, University of Cambridge, Cambridge CB2 1LR, United Kingdom

^bHoward Hughes Medical Institute and Division of Biology and Biological Engineering, California Institute of Technology, Pasadena, California 91125

^cState Key Laboratory for Conservation and Utilization of Subtropical Agrobioresources, South China Agricultural University, Guangzhou 510642, China

ORCID IDs: 0000-0002-2379-5729 (W.Y.); 0000-0002-1948-2367 (C.S.); 0000-0002-8939-5920 (N.P.); 0000-0002-2371-9996 (B.L.); 0000-0003-1295-4875 (R.W.); 0000-0003-4798-5153 (E.M.M.).

In addition to transcriptional regulation, gene expression is further modulated through mRNA spatiotemporal distribution, by RNA movement between cells, and by RNA localization within cells. Here, we have adapted RNA fluorescence in situ hybridization (FISH) to explore RNA localization in *Arabidopsis* (*Arabidopsis thaliana*). We show that RNA FISH on sectioned material can be applied to investigate the tissue and subcellular localization of meristem and flower development genes, cell cycle transcripts, and plant long noncoding RNAs. We also developed double RNA FISH to dissect the coexpression of different mRNAs at the shoot apex and nuclear-cytoplasmic separation of cell cycle gene transcripts in dividing cells. By coupling RNA FISH with fluorescence immunocytochemistry, we further demonstrate that a gene's mRNA and protein may be simultaneously detected, for example revealing uniform distribution of *PIN-FORMED1* (*PIN1*) mRNA and polar localization of PIN1 protein in the same cells. Therefore, our method enables the visualization of gene expression at both transcriptional and translational levels with subcellular spatial resolution, opening up the possibility of systematically tracking the dynamics of RNA molecules and their cognate proteins in plant cells.

¹This work was funded by the Gatsby Charitable Foundation (through fellowship GAT3395/DAA). E.M.M. is supported by the Howard Hughes Medical Institute. The Microscopy and Histology Facilities at the Sainsbury Laboratory are supported by The Gatsby Charitable Foundation. Q.D. is supported by the Graduate Student Oversea Study Program South China Agricultural University (2018LHPY011).

²Present address: Department of Molecular, Cell, and Developmental Biology, University of California, Los Angeles, Los Angeles, CA 90095

³Present address: Laboratoire Reproduction et Développement des Plantes, Université de Lyon, Ecole Normale Supérieure de Lyon, UCB Lyon 1, Centre National de la Recherche Scientifique, Institut National de la Recherche Agronomique, 69342 Lyon cedex 07, France.

⁴Author for contact: meyerow@caltech.edu.

⁵Senior author.

The author responsible for distribution of materials integral to the findings presented in this article in accordance with the policy described in the Instructions for Authors (www.plantphysiol.org) is: Elliot M. Meyerowitz (meyerow@caltech.edu).

W.Y. and E.M.M. designed the research; W.Y. performed most of the experiments; C.S. helped to generate some of the probes; N.P., Q.D., and B.L. carried out fluorescent reporter analysis; W.Y. and E.M.M. analyzed the data and wrote the article with contributions from R.W. and C.S.

^[OPEN]Articles can be viewed without a subscription.

www.plantphysiol.org/cgi/doi/10.1104/pp.19.00980

With the rapid development of sequencing technologies and continuing reduction in sequencing cost, a growing number of plant genome sequences are being released, and de novo assembly of model and nonmodel plant genomes is becoming feasible for individual research groups (Jiao and Schneeberger, 2017; Michael et al., 2018). Determining when, where, and how the genes are expressed should provide important insight into gene function. The expression of individual genes can be assessed by reverse transcription quantitative PCR. Microarray and RNA sequencing allow the examination of gene expression at the whole transcriptome level. Whereas these methods generate comprehensive quantitative information, they do not reveal the detailed spatial patterns of RNA distribution.

Determining the spatiotemporal gene expression dynamics is of particular importance in plant developmental biology (Schmid et al., 2005). Local activation of gene expression, together with the precisely controlled intercellular trafficking of proteins, gives rise to distinct landscapes of growth regulators that coordinate stem cell maintenance, cell division and differentiation, and ultimately organogenesis (Rogers and Schier, 2011; Xu et al., 2011; Yadav et al., 2011). In *Arabidopsis* (*Arabidopsis thaliana*), the precise locations

of WUSCHEL (WUS) and CLAVATA3 (CLV3) proteins, distinct from the locations of their mRNAs in the shoot apical meristem (SAM), define a regulatory circuit essential for meristem homeostasis (Brand et al., 2000; Schoof et al., 2000). Small RNAs, expressed in various tissues such as root tips and leaves, can move from their sites of synthesis to distant regions, generating a molecular gradient that governs cell fate acquisition and tissue polarity establishment (Chitwood et al., 2009; Carlsbecker et al., 2010; Zhu et al., 2011; Skopelitis et al., 2017).

Promoter-driven reporter gene expression is a widely used technique to depict gene expression in plants. The coding sequences of enzymes (such as GUS) or fluorescent proteins are inserted downstream of the target gene promoters, and the transcriptional activities are evaluated by tracking the enzymatic reaction or fluorescence. Reporter gene analysis, when combined with genetic and molecular assays, has greatly facilitated the functional study of genes. However, due to the stability of fluorescent proteins and the potential diffusion of GUS staining products and GFP, promoter reporters sometimes do not fully reflect the RNA distribution, and they fail to reveal any posttranscriptional regulation that may occur that is dependent on the coding regions of the gene's mRNA. In addition, the construction of reporter lines involves gene transformation, which is time-consuming, especially in crops, and can only be achieved in a limited number of plant models. Alternatively, RNA in situ hybridization (ISH) has been deployed to investigate gene expression. Target RNAs are recognized by in vitro-transcribed antisense RNA probes. The probes are labeled with small molecular tags that can be detected by enzyme-conjugated antibodies. The specificity of probe binding enables the precise location of target gene transcripts in a wide range of species as well as in different plant organs.

RNA abundance is highly variable between tissues or even between the same cell types in a single tissue. RNA subcellular localization has been shown to play important roles in the control of gene function. To determine RNA localization at the cellular level, fluorescence in situ hybridization (FISH) was developed and has become a vital tool in analyzing animal and yeast gene expression (Levsky and Singer, 2003). In plants, FISH has been used to visualize entire chromosomes or individual genetic loci (Lamb et al., 2007; Tirichine et al., 2009; Jiang, 2019) as well as pathogen DNA (Shargil et al., 2015). However, although there are notable examples using whole-mounted tissues (Bruno et al., 2011, 2015; Himanen et al., 2012; Rozier et al., 2014; Bleckmann and Dresselhaus, 2016; Woloszynska et al., 2019), the use of FISH to investigate plant RNA localization at high resolution and deep in tissues remains to be fully exploited. We have established RNA FISH in the Arabidopsis shoot apex based on the tyramide signal amplification (TSA) system applied to sectioned tissue (Yang et al., 2017). We have shown that this RNA FISH method, when coupled with cell wall or nuclear counterstaining, allows detection of the locations of

RNA molecules in individual cells. Here, we provide step-by-step protocols showing how mRNAs of different genes can be concurrently analyzed through double RNA FISH, and we combine RNA FISH with immunofluorescence to visualize both mRNA and the corresponding protein within the same sample. We demonstrate these techniques by mapping the mRNA distribution and coexpression of flower development genes, investigating a novel family of nuclear mRNAs, and exploring the correlation of *PIN-FORMED1* (*PIN1*) transcription and protein polarization in thick shoot tissues.

RESULTS

Establishment of RNA FISH in Arabidopsis

In conventional ISH, the colorimetric reactions on chromogenic substrates are usually catalyzed by alkaline phosphatase. To improve the resolution, we developed methods for RNA FISH in plants. We proposed that a feasible strategy would meet the following criteria: (1) specificity: fluorescence signals need to reliably reflect the localization of target RNA molecules; (2) sensitivity: variation in gene expression levels requires a flexible detection method that is suitable for both high- and low-abundance transcripts; and (3) scalability: such a method should be achievable for examining and comparing multiple transcripts in a cost- and time-effective manner.

To achieve these goals, we adapted and optimized the TSA system (van de Corput et al., 1998). In this approach, target RNA molecules are hybridized with digoxigenin- or fluorescein-labeled probes, which are further recognized by horseradish peroxidase-conjugated antibodies specific to digoxigenin and fluorescein. Subsequently, peroxidase-catalyzed reactions lead to the covalent binding of fluorochrome-labeled tyramides to proteins (i.e. the antibodies) that are in close proximity to the probes, thereby providing a precise way to label target RNA molecules (Fig. 1A). This signal amplification process also enables the sensitive detection of transcripts with relatively low abundance. The TSA system has been applied in whole-mount ISH to detect gene expression in Arabidopsis seedlings, embryos, and shoot apices (Bruno et al., 2011; Himanen et al., 2012; Rozier et al., 2014; Woloszynska et al., 2019). By incorporating TSA into standard RNA ISH procedures using sectioned material to allow high-resolution visualization even deep in tissues, we constructed a pipeline for investigating gene expression and coexpression (Fig. 1B). To assess the specificity and sensitivity of RNA FISH, we first examined the expression of *WUS* and *HISTONE H4* (*HIS4*) mRNAs in Arabidopsis shoot apices. *WUS* encodes a homeodomain transcription factor expressed in a small group of cells within the SAM and flower primordia, which defines the upper part of the rib meristem (Mayer et al., 1998). *HIS4* is transcribed during DNA replication, and

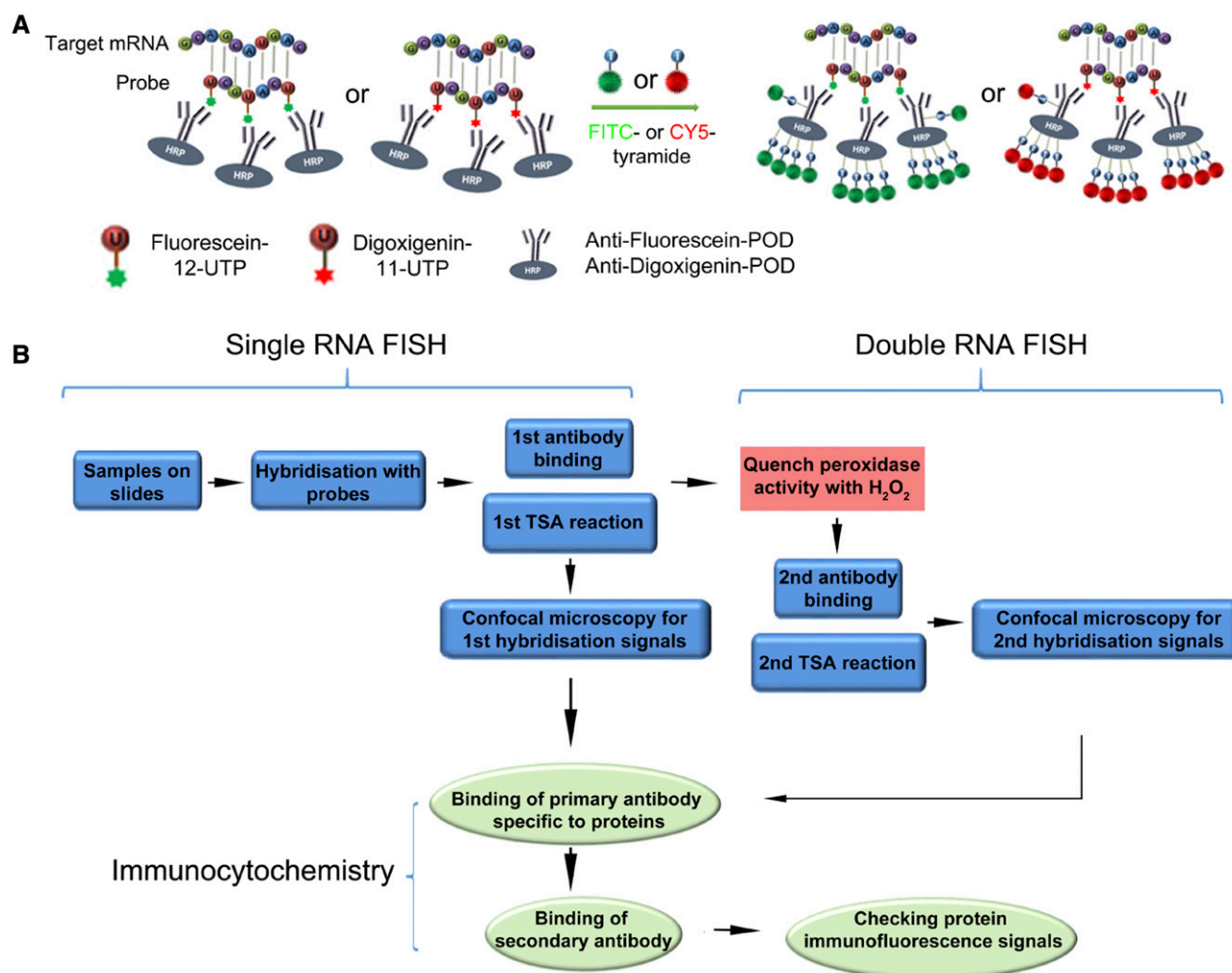


Figure 1. Overview of the RNA FISH coupled with protein immunofluorescence. A, Schematic representation of RNA ISH and signal detection using the TSA system. FITC, Fluorescein; HRP, horseradish peroxidase; POD, peroxidase. B, Flow chart showing the major steps for concurrent detection of multiple RNAs together with proteins.

its mRNAs are only present in cells at the S-phase of the cell cycle (Sorrell et al., 1999). The hybridization signals of *WUS* and *HIS4* RNA FISH were similar to those seen using chromogenic ISH (Supplemental Fig. S1, A, B, D, and E) and were also consistent with the expression of *WUS* and *HIS4* promoter fluorescent reporters (Supplemental Fig. S1, C and F), indicating that RNA FISH could detect both tissue- and cell type-specific mRNAs in plants.

RNA FISH to Reveal the Expression of Developmental Genes in the Shoot Apex

Arabidopsis shoot apex development is coordinated by a number of transcription factors that are expressed in well-defined domains (Fig. 2A; Bowman et al., 1991). We combined RNA FISH with fluorescent dyes to visualize the cellular distribution of RNAs involved in meristem and early flower development (Supplemental

Figs. S2 and S3). Calcofluor White, a water-soluble dye that binds to cell wall components, was used to label cell boundaries (Supplemental Fig. S2A). *WUS* mRNA was found localized underneath the L2 layer of the SAM (Fig. 2B), and *CLV3* transcripts accumulated in the central zone (Fig. 2C), in accordance with the literature (Mayer et al., 1998; Fletcher et al., 1999). In contrast to *WUS*, *SHOOT MERISTEMLESS (STM)*, another homeodomain transcription factor (Clark et al., 1996; Long et al., 1996), showed strong and ubiquitous expression across the SAM but was only weakly expressed or not expressed at all in new and early-stage flower primordia (Fig. 2D).

Continuous division of stem cells in the central zone generates progenitor cells that are displaced toward the peripheral zone, giving rise to flower primordia (Meyerowitz, 1997). *APETALA1 (AP1)* and *LEAFY (LFY)* are floral meristem identity genes (Weigel et al., 1992; Bowman et al., 1993; Mandel et al., 1995; Blázquez et al., 1997), which are expressed in early-stage

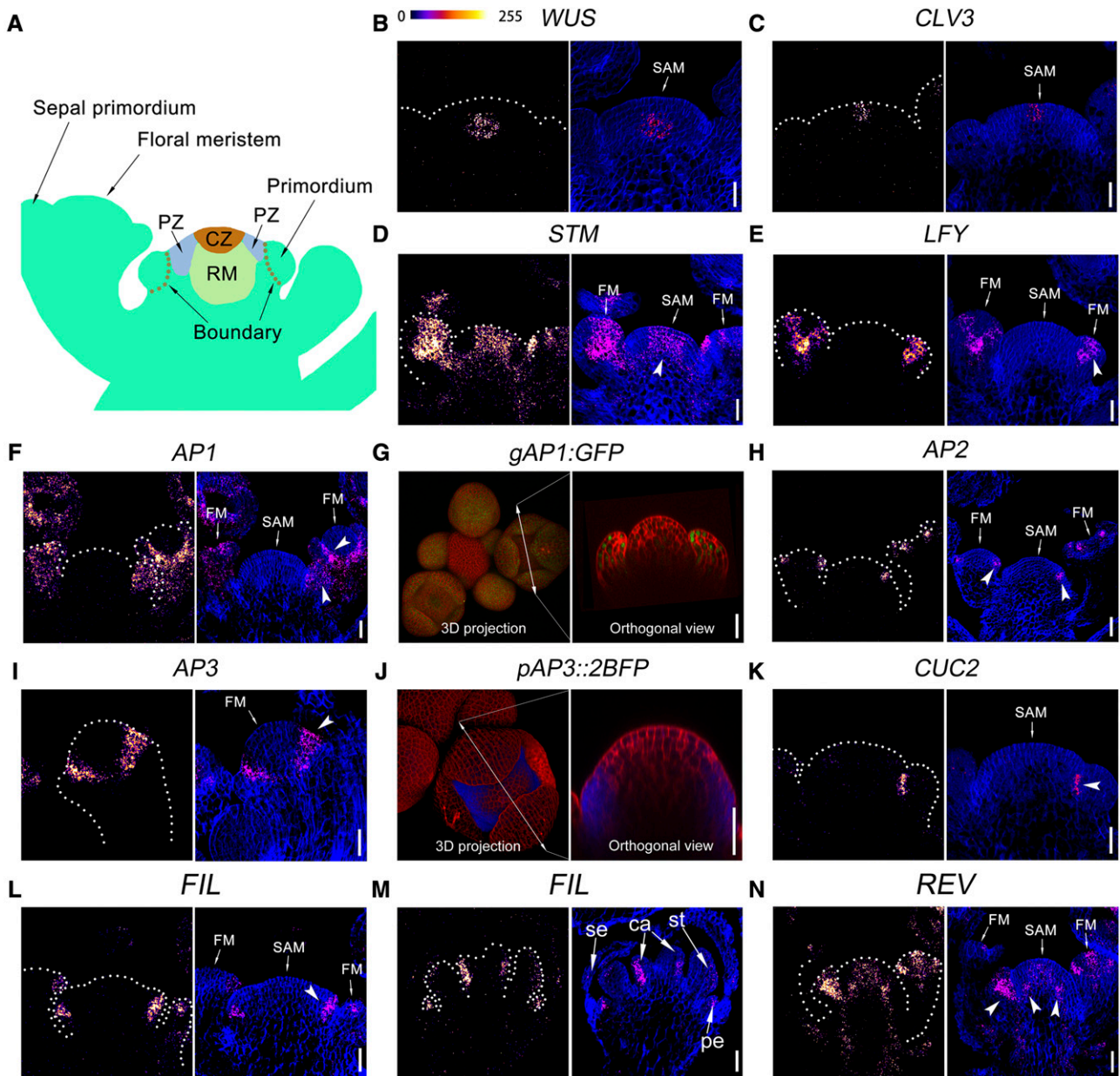


Figure 2. mRNA expression patterns of meristem and flower development genes revealed by RNA FISH. The mRNAs (magenta) were hybridized with digoxigenin-labeled antisense RNA probes and detected by TSA-Cy5. Cell walls were stained by Calcofluor White and are shown in blue. Left images show RNA FISH signals in a Fire format. Meristems and flowers are outlined by white dashed lines. A, Schematic representation of the Arabidopsis inflorescence shoot apex. CZ, Central zone; PZ, peripheral zone; RM, rib meristem. B to F, H, K, L, and N, The distribution of *WUS* mRNA in the shoot apex (B), *CLV3* (C), *STM* (D), *LFY* (E), *AP1* (F), *AP2* (H), *CUC2* (K), *FIL* (L), and *REV* (N). I, *AP3* mRNA expression in a stage 3 flower. M, *FIL* mRNA expression in a stage 6 flower. ca, Carpel; pe, petal; se, sepal; st, stamen. G and J, Expression patterns of *AP1* translational fusion reporter *gAP1::GFP* (Urbanus et al., 2009) in the shoot apex and *AP3* transcriptional reporter *pAP3::2BFP* in a stage 4 flower. Shown are 3D projections of confocal stacks. The cell walls are stained with propidium iodide (in red). Left images show top view and right images show side view. FM, Floral meristems. RNA FISH signals are indicated with arrowheads. See Supplemental Figure S3 for serial sections. Bars = 25 μ m.

flowers (Fig. 2, E–G). Whereas *AP1* was expressed uniformly in stage 2 flower primordia, *LFY* mRNA was enriched in the inner four layers of cells. At later stages (stage 3), both *AP1* and *LFY* mRNAs were absent from the inner whorls (Fig. 2, E and F). *AP2* functions as an

A-class organ identity gene conferring sepal and petal identity (Bowman et al., 1991; Jofuku et al., 1994). Consistently, *AP2* was transiently expressed in sepal primordia (Fig. 2H). *AP2* also cooperates with B-class genes such as *AP3* in the second whorl (Krizek and

Meyerowitz, 1996). In agreement with this, both *AP2* and *AP3* mRNAs appeared in stamen and petal primordia (Fig. 2, H–J), and some of the *AP3* transcript was detected in the inner parts of early sepals (Fig. 2I).

The SAM and the newly formed flower primordia are separated by a group of less-proliferative cells that specify the boundary domain. Boundary formation is controlled by a family of NAC transcription factors including *CUP-SHAPED COTYLEDON1* (*CUC1*), *CUC2*, and *CUC3* (Aida et al., 1997). Examination of *CUC2* expression revealed fluorescence signals restricted to one to two lines of cells between the SAM and the flower primordia (Fig. 2K).

We also examined genes that exhibit asymmetric expression patterns in organs, such as *FILAMENTOUS FLOWER* (*FIL*) and *REVOLUTA* (*REV*), coding for a zinc finger and HMG box-like domain transcription factor (Sawa et al., 1999) and a homeodomain Leu zipper transcription factor (Otsuga et al., 2001), respectively. In both early primordia and developed flowers, *FIL* mRNAs were expressed in cells on the abaxial side of the organs (Fig. 2, L and M). In contrast, *REV* transcripts were enriched on the adaxial side of the young primordia and showed an inverted cup-shaped distribution in the center of the SAM (Fig. 2N).

Taken together, with RNA FISH, we could detect the mRNAs of genes with variable expression levels. The distribution patterns revealed by RNA FISH were similar to those from conventional chromogenic ISH and were also consistent with transgenic fluorescence reporters.

Investigating Gene Coexpression by Double RNA FISH

Determining the coexpression patterns of genes can provide important insights into their genetic and molecular functions. Standard ISH allows for the examination of different transcripts separately. In TSA RNA FISH, the hybridization signals are revealed by a peroxidase-catalyzed reaction. As peroxidase activity can be quenched by hydrogen peroxide (H_2O_2) treatment, TSA RNA FISH enables sequential detection of different mRNAs in the same sample (Supplemental Fig. S1B). *STM* expression declined when flower primordia emerged (Fig. 2D), and primordium formation was accompanied by the acquisition of *ARABIDOPSIS HISTIDINE PHOSPHOTRANSFER PROTEIN6* (*AHP6*) expression (Bartrina et al., 2011; Besnard et al., 2014; Supplemental Fig. S4A). *AHP6* encodes a pseudophosphotransfer protein involved in the inhibition of cytokinin signaling (Mähönen et al., 2006). Similar to the fluorescent reporter, *AHP6* mRNAs were highly enriched in early primordia (Supplemental Fig. S4B). By double RNA FISH, we investigated the coexpression of *STM* and *AHP6* mRNAs within the same meristem, showing complementary distributions (Fig. 3A).

In developing flowers, both *AP3* and *AHP6* expression coincided with the formation of floral organs and their mRNAs appeared to be localized in similar domains (Figs. 2I and 3A; Supplemental Fig. S4B).

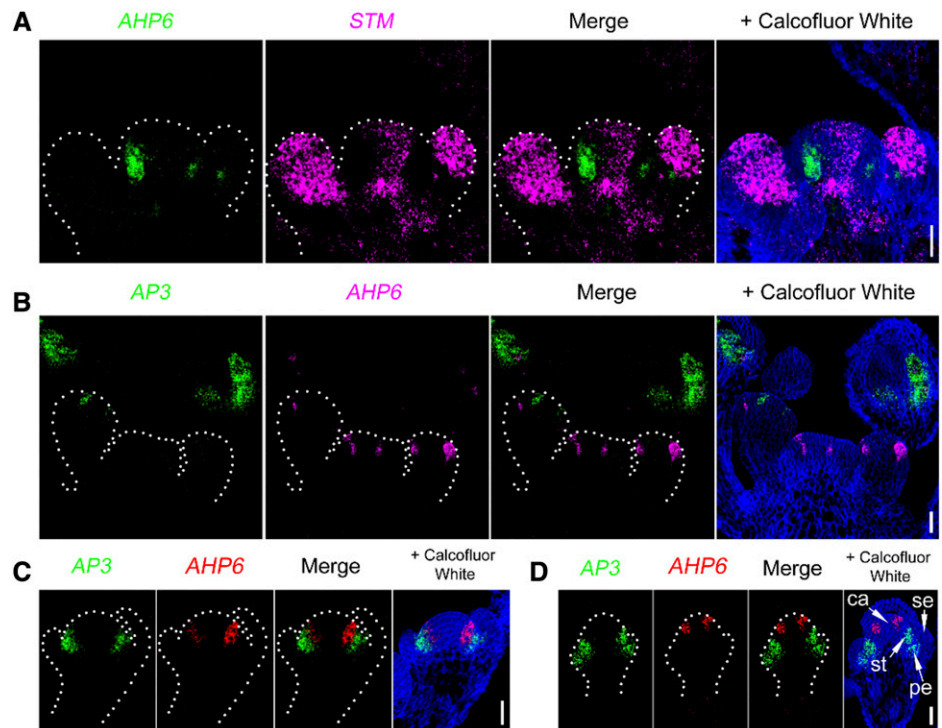
However, in double RNA FISH, we found few cells that contained both transcripts (Fig. 3B). Instead, in a majority of the cells, *AP3* expression was restricted to the stamen and petal primordia and *AHP6* mRNAs were expressed in two layers of cells inside the *AP3* expression domain (Fig. 3, C and D), reminiscent of the codistribution of *SUP3* and *AP3* mRNAs (Prunet et al., 2017). In summary, single and double RNA FISH revealed distinct expression domains of meristem and flower development genes, providing high-resolution gene coexpression patterns.

Localization of Nuclear and Cytoplasmic mRNAs

To further evaluate the sensitivity of RNA FISH in detecting highly localized transcripts at the single-cell level, we analyzed the expression of the cell cycle gene *CYCLIN-DEPENDENT PROTEIN KINASE1;2* (*CYCB1;2*) in the SAM. Similar to *HIS4* (Fig. 1E), we observed nonhomogeneously distributed fluorescence signals of *CYCB1;2* mRNAs in RNA FISH (Supplemental Fig. S5A). To define at which stages *HIS4* and *CYCB1;2* are expressed, we coupled RNA FISH with 4',6-diamidino-2-phenylindole (DAPI) staining. DAPI is a fluorescent dye that specifically binds to DNA and thereby can be used to monitor the morphological changes of the chromosomes during cell division. *CYCB1;2* mRNAs were found to be present in prophase, prometaphase, and metaphase cells but not in later stages of the cell cycle (Supplemental Fig. S5B), consistent with its transient expression at the G2-to-M phase transition. On the other hand, *HIS4* RNA was present during DNA replication at S phase, and its mRNA was distributed in cells with intact nuclei (Supplemental Fig. S5C). The sequential expression of *HIS4* and *CYCB1;2* during the cell cycle was further investigated by double RNA FISH. Using probes with different tags, we show that *CYCB1;2* is expressed exclusively in mitotic cells, and *HIS4* mRNAs are detected in another group of cells that do not overlap with *CYCB1;2*-expressing cells (Fig. 4).

Whereas most of the RNAs we analyzed are localized in the cytoplasm, we previously identified two mRNAs, from the genes *CDC20* and *CCS52B*, that are specifically localized inside the nucleus during prophase (Yang et al., 2017). *CDC20* and *CCS52B* are activators of the anaphase-promoting complex/cyclosome (APC/C) that promotes anaphase onset during cell division (Yu, 2007). In animals, *CDC20* proteins are sequestered by the mitotic checkpoint complex (MCC), which in turn inhibits APC/C activity during early mitosis (Izawa and Pines, 2015). We found that in Arabidopsis, all MCC components, *MAD2*, *BUB3*, and *BUBR1*, were specifically expressed in mitotic cells together with *CYCB1;1* and their mRNAs were all exported into the cytoplasm (Fig. 5A; Supplemental Fig. S6). *CDC20* was coexpressed with *MAD2*, but its mRNA was restricted to the inside of the nucleus, which prevents protein translation (Yang et al., 2017; Fig. 5B). Hence, even

Figure 3. Double RNA FISH to show the spatial separation of different mRNAs. Gene-specific probes were labeled with digoxigenin or fluorescein isothiocyanate (FITC) and detected by TSA-Cy5 (magenta signals) or TSA-FITC (green signals), respectively. A, SAM overview showing the expression patterns of primordia-specific *AHP6* mRNA with meristem-expressed *STM* mRNA. B, Expression patterns of *AP3* and *AHP6* in the same tissue section of the shoot apex. C and D, Spatial separation of *AP3* and *AHP6* mRNAs in stage 4 (C) and stage 5 (D) flowers. ca, Carpel; pe, petal; se, sepal; st, stamen. Bars = 25 μ m.



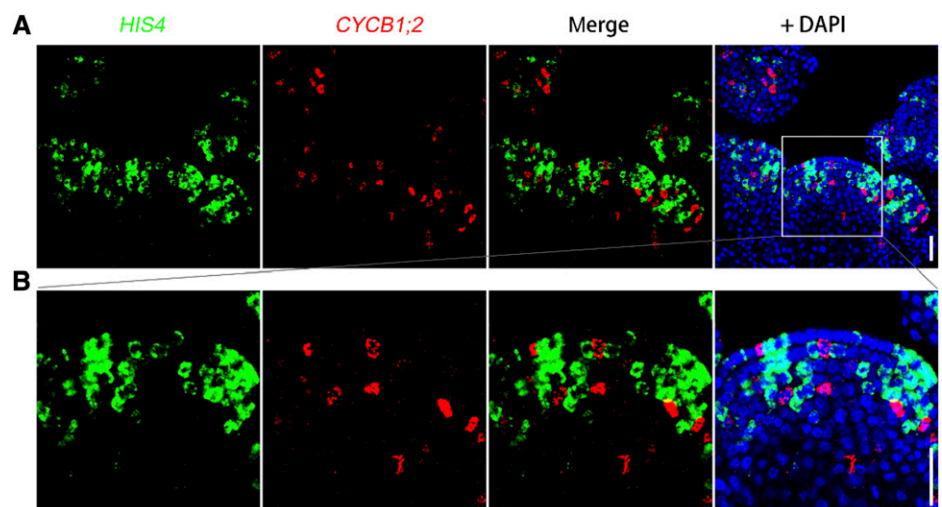
without MCC-mediated inhibition, this mRNA nuclear localization would be sufficient to prevent premature APC/C activation.

Detection of Long Noncoding RNA

Recently, a number of long noncoding RNAs (lncRNAs) have been identified in plants, including natural antisense transcripts (NATs; Wang et al., 2014). The sequences of NAT-lncRNAs overlap with protein-coding mRNAs, but they are transcribed from the opposite direction. The 5' region of the nuclear mRNA *CCS52B* includes a NAT-lncRNA. We named this

previously uncharacterized transcript as *lncRNA^{CCS52B}* (Fig. 6A). To assess whether RNA FISH can be used to examine lncRNA localization in plants, we analyzed the spatial distribution of *lncRNA^{CCS52B}* transcripts. A pair of 376-bp RNA probes fully complementary with each other was designed to recognize *CCS52B* and *lncRNA^{CCS52B}*, respectively. Consistent with our previous results (Yang et al., 2017), *CCS52B* mRNAs were found to localize inside the nucleus of mitotic cells (Fig. 6B). By contrast, *lncRNA^{CCS52B}* expression was absent from proliferating cells both in the SAM and in flower primordia. Instead, we detected strong fluorescence signals in the pedicel of early-stage flowers (Fig. 6C). These results suggest that coding mRNAs and

Figure 4. Detection of cell cycle gene mRNAs in individual meristem cells. A, *HIS4* probe was labeled with fluorescein isothiocyanate (FITC) and detected by TSA-FITC (green signals). *CYCB1;2* probe was labeled with digoxigenin and detected by TSA-Cy5 (red signals). *HIS4* and *CYCB1;2* mRNAs were observed in different cells, indicating a nonoverlapping expression pattern during the cell cycle. B, Enlargement of the region outlined in A. The nucleus (blue) was labeled by DAPI staining. Bars = 25 μ m.



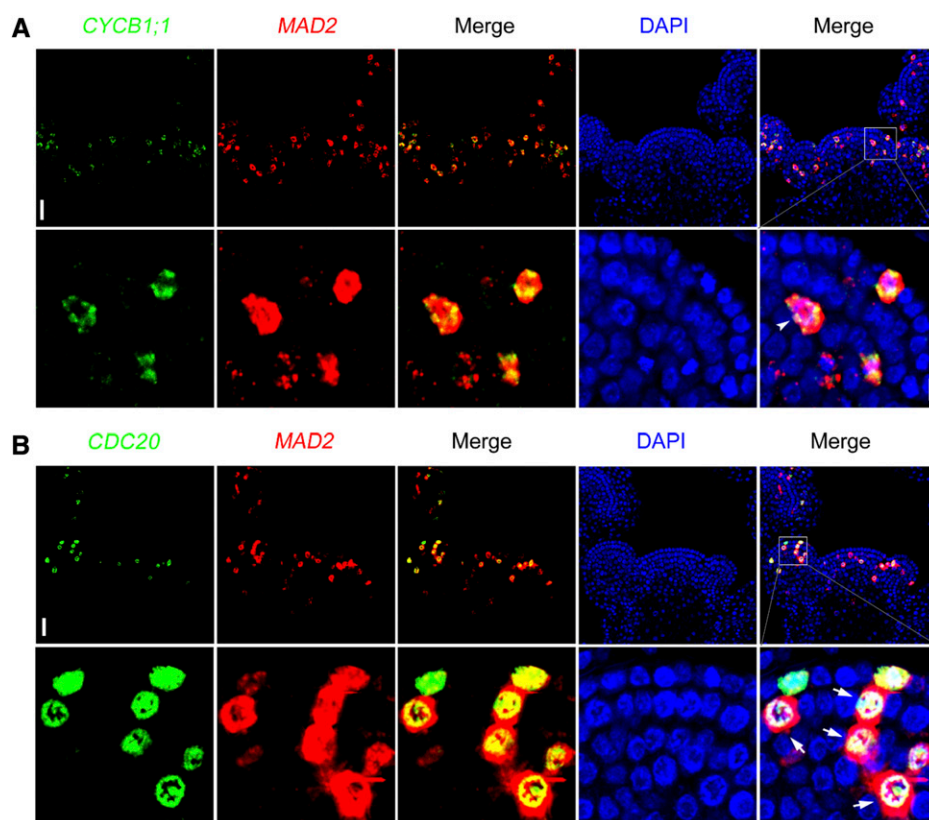


Figure 5. Subcellular localization of cell cycle mRNAs in the cytoplasm and the nucleus. *CYCB1;1* and *CDC20* probes were labeled with fluorescein isothiocyanate (FITC) and detected by TSA-FITC (green signals). *MAD2* probe was labeled with digoxigenin and detected by TSA-Cy5 (red signals). **A**, Colocalization of *CYCB1;1* and *MAD2* mRNAs in the cytoplasm of mitotic cells. The arrowhead indicates a prophase cell that expresses *CYCB1;1* and *MAD2*. **B**, Nucleocytoplasmic separation of *CDC20* and *MAD2* mRNAs in the same cells. Arrows indicate prophase cells that coexpress *CDC20* and *MAD2*. *CDC20* mRNAs are retained in the nucleus, whereas *MAD2* mRNAs are exported into the cytoplasm. The bottom row shows enlargement of the regions outlined in the top row. Bars in top rows = 25 μm and bars in bottom rows = 10 μm .

their antisense noncoding transcripts may exhibit divergent expression patterns, perhaps due to different upstream regulatory sequences. The lncRNAs function in both the nucleus and the cytoplasm, and in the cytoplasm a large proportion of lncRNAs associate with ribosomes, possibly being involved in development and response to environmental cues (Jiao and Meyerowitz, 2010; Bazin et al., 2017). We found that *lncRNA^{CC52B}* RNAs were predominantly localized in the cytoplasm (Fig. 6C), suggesting possible structural or regulatory functions in translation or RNA stability.

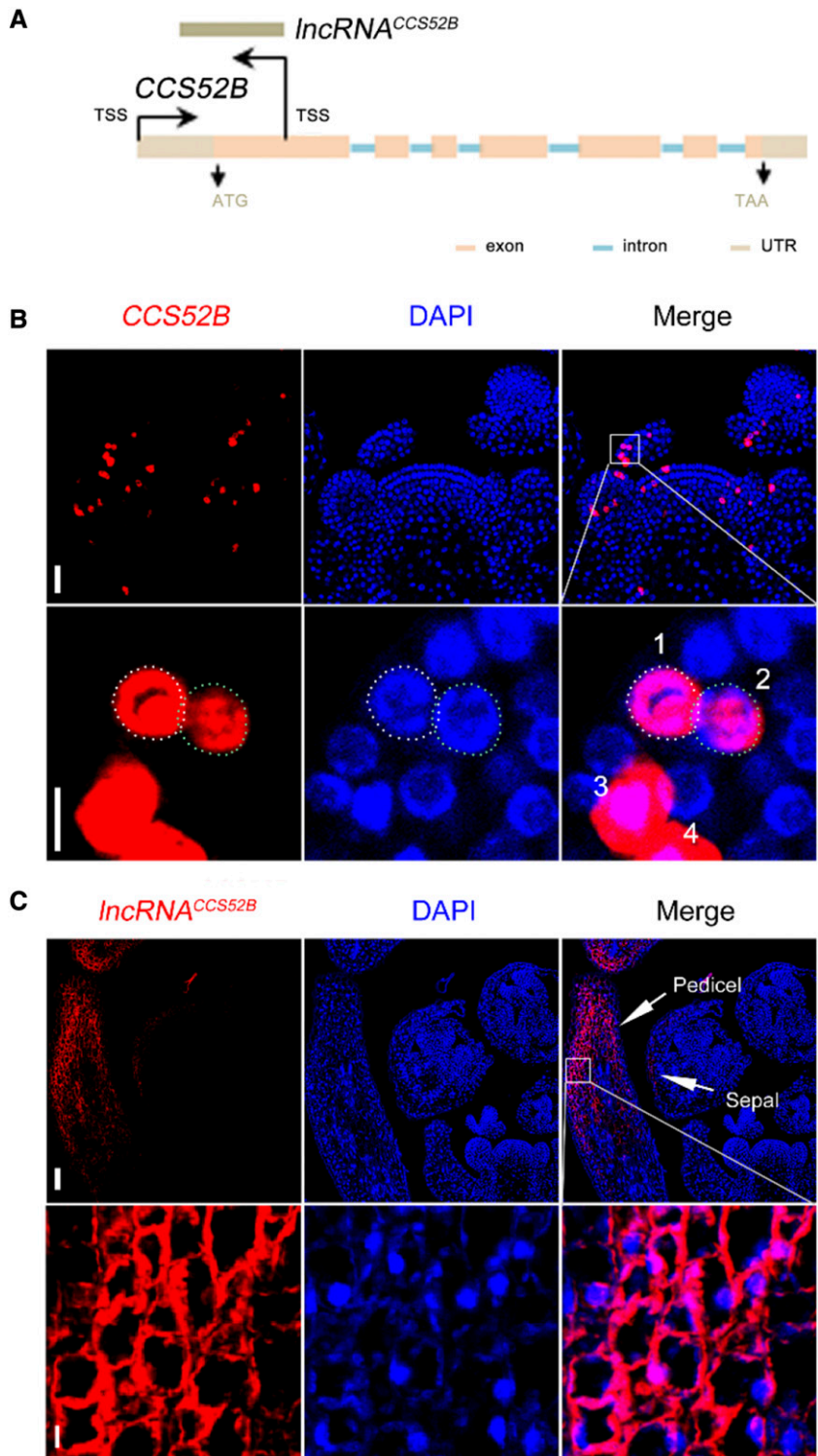
Simultaneous Observation of Auxin Transporter *PIN1* mRNA and PIN Protein by RNA FISH and Immunofluorescence

Determining protein cellular and subcellular localization in combination with mRNA expression would be informative in elucidating the transcriptional and posttranslational regulation of genes and could serve as a clue to biological function. To do this, we optimized the protein immunofluorescence protocol (see “Materials and Methods”) and incorporated it into the RNA FISH, leading to a pipeline that enables examination of both mRNA and protein in the same tissue section (Supplemental Fig. S1B). We tested this in the shoot apex by monitoring *PIN1* mRNA and PIN1 protein expression. *PIN1* encodes an auxin efflux carrier involved in polar auxin transport (Gälweiler et al.,

1998). Live imaging of the *PIN1* fluorescent reporter *PIN1::PIN1-GFP* has revealed dynamic PIN1 polarity changes during primordium formation in the shoot apex (Heisler et al., 2005). We found that when PIN1-GFP was observed by immunofluorescence using an anti-GFP antibody, localization patterns similar to fluorescent reporter live imaging were revealed (Fig. 7). In the central part of the meristem, PIN1-GFP protein was mainly detected in L1 cells, whereas under flower primordia, its expression extended to deeper cell layers (Fig. 7A). In line with the protein distribution, *PIN1* mRNA was also enriched in the L1 layer of meristem cells and in the primordia (Fig. 7A; Supplemental Fig. S7, A and B). In individual cells of the primordium, PIN1-GFP exhibited a polar localization, whereas *PIN1* mRNA was uniformly distributed in the cytoplasm (Fig. 7A, bottom row), in agreement with posttranslational establishment of polarity.

Due to the limitation of scanning depth, PIN1-GFP fluorescence signals deep in thick tissues such as stems are difficult to image by confocal microscopy (Supplemental Fig. S7C) or by whole-mount FISH. However, with immunofluorescence on longitudinal sections, PIN1 proteins could be readily observed and localized with high resolution in deep regions of the shoots. Compared with the SAM, both *PIN1* mRNA and PIN1 protein expression were much more abundant in vascular cells (Fig. 7A). Auxin-signaling output, as evaluated by GFP RNA FISH and protein immunofluorescence expressed under the control of an auxin-responsive

Figure 6. Detection of an lncRNA by RNA FISH. A, Schematic representation of *CCS52B* and its antisense lncRNA *lncRNA^{CCS52B}*. *CCS52B* and *lncRNA^{CCS52B}* are transcribed from the same genomic region but with opposite directions. TSS, Transcription start site; UTR, untranslated region. B, Nuclear localization of *CCS52B* mRNA in dividing cells. Cells 1 and 2 in the bottom row are prophase cells in which *CCS52B* mRNAs are localized inside the nucleus. The nuclear boundaries are labeled with dashed lines. Cells 3 and 4 are metaphase cells without nuclear envelopes, and *CCS52B* mRNAs are released into the cytoplasm. Bar in top row = 25 μm and bar in bottom row = 5 μm . C, Expression of *lncRNA^{CCS52B}* was observed in sepal and pedicel of young flowers. Bar in top row = 50 μm and bar in bottom row = 5 μm . The bottom rows in B and C are enlarged views of the regions outlined in the top rows.



promoter (DR5-n3GFP; Liao et al., 2015), was also highly enriched in the vasculature (Supplemental Fig. S8, A–C) as well as in cells at the top of the ovule and stamen primordia (Supplemental Fig. S8, D and E). Whereas the mRNA FISH signals were generally consistent with the protein immunofluorescence, we also found a number of cells that only contained GFP protein but without RNA

FISH signals (Supplemental Fig. S8B), possibly due to perdurance of the stable GFP protein.

DISCUSSION

Whole-genome transcript profiling has provided comprehensive information about RNA abundance in

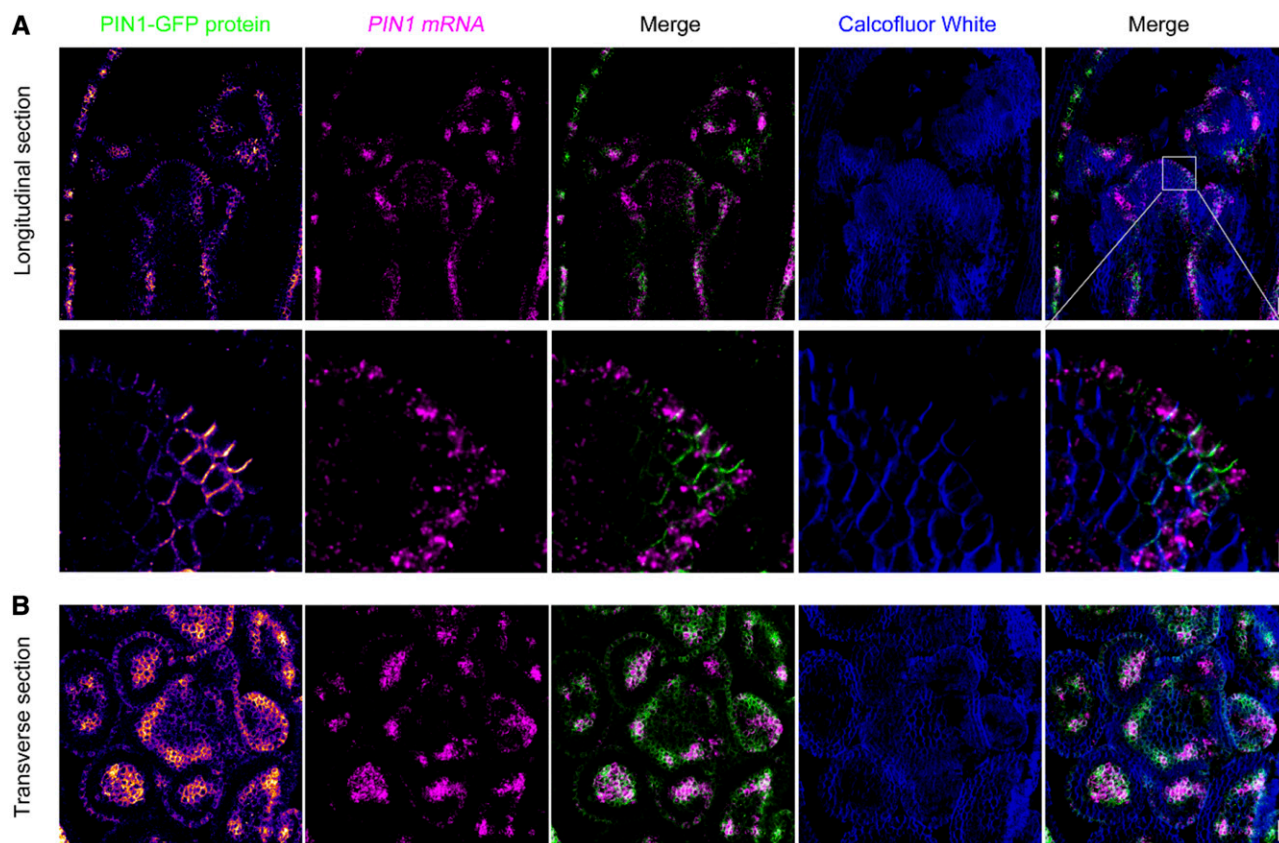


Figure 7. Coexpression of PIN1-GFP protein and *PIN1* mRNA in the shoot apex. PIN1-GFP protein was detected by immunofluorescence using an anti-GFP antibody. *PIN1* mRNA was revealed by RNA FISH. PIN1-GFP protein immunofluorescence signals are shown in Fire format. A, Distribution of PIN1 protein and *PIN1* mRNA in longitudinal sections of the shoot apex. The bottom row shows enlarged views of the region outlined in the top row to reveal the polarization of PIN1-GFP protein and cytoplasmic localization of *PIN1* mRNA in meristem cells. Bar in top row = 20 μm and bar in bottom row = 5 μm . B, Distribution of PIN1 protein and mRNA in transverse sections of the shoot apex. Bar = 20 μm .

various plant tissues and has revealed gene expression dynamics in response to environmental signals. To further unravel the functions of coding and noncoding transcripts, it is necessary to resolve their distribution at the single cell and subcellular levels. Single-cell RNA sequencing has been recently applied in plants to resolve transcriptome dynamics in different root cell types (Denyer et al., 2019; Jean-Baptiste et al., 2019; Ryu et al., 2019; Shulze et al., 2019; Zhang et al., 2019). However, only some genes are expressed in a cell type-specific manner (consider cell cycle-expressed genes as a counterexample), and these methods do not yet, at least, resolve subcellular locations of RNA molecules. As an alternative strategy, we have adapted RNA FISH to investigate gene expression in Arabidopsis. The results demonstrate that gene expression patterns revealed by RNA FISH are comparable to those generated by standard chromogenic RNA ISH, but with higher cellular and subcellular resolution.

mRNA expression patterns help with the interpretation of genetic and molecular interactions between genes involved in the same developmental or physiological pathways (Stuart et al., 2003). Gene coexpression

can be analyzed by comparing transcript abundance in the same tissues or by examining mRNA distribution through ISH in different samples. These techniques do not provide the simultaneous localization of different mRNAs in the same cells. We show that double RNA FISH enables the simultaneous detection of multiple genes' transcripts in the same samples. Through nuclear staining by DAPI, together with double RNA FISH, we identified a pair of mRNAs, namely *CDC20* and *CCS52B*, that are coexpressed with their regulatory MCC component genes as well as their target *Cyclin B* genes (Yang et al., 2017); whereas MCC genes and *Cyclin B* mRNAs are normally exported into cytoplasm, *CDC20* and *CCS52B* mRNAs are found inside the nucleus during prophase. mRNA nuclear retention blocks protein translation, thus providing a new mechanism for gene expression control and plant cell division regulation.

In addition, both mRNA and its corresponding protein can be simultaneously analyzed in the same cells by RNA FISH coupled with protein immunofluorescence. As an example, we show a uniform distribution of *PIN1* mRNA and polarization of PIN1 protein in the same

epidermal cells of the SAM. We also show that *PIN1* mRNA and PIN protein can be visualized in thick tissues of the stem, revealing a high expression of PIN1 along the vasculature (Fig. 7B). The RNA FISH and immunofluorescence data generated by fluorescence or confocal microscopy can be measured, at least relatively. When combined with cell and nuclear shape segmentation, and proper quantitative controls, this approach could have applications in quantifying the relative amount of mRNAs and proteins for systematic cell biological analysis in plants (Rhee et al., 2019). Using RNA FISH, we could analyze the mRNA expression of most genes. However, when the transcripts per kilobase million value of one transcript was below 10 in dissected tissue RNA sequencing experiments, it was difficult to detect clear hybridization signals. Therefore, to fully reveal the mRNA abundance and subcellular localization, we may need to consider both ISH and high-throughput sequencing strategies.

MATERIALS AND METHODS

Plant Materials and Growth Conditions

Arabidopsis (*Arabidopsis thaliana*) Columbia ecotype was used as the wild-type control for gene expression analysis. The reporter lines *pWUS::GFP*, *H4::DB-VENUS*, *pAP3::2BFP*, *gAPI::GFP*, *PIN1::PIN1-GFP*, and *DR5-n3GFP* were described previously (Benková et al., 2003; Jönsson et al., 2005; Urbanus et al., 2009; Liao et al., 2015; Jones et al., 2017). Seeds were germinated on Murashige and Skoog (MS) agar plates, and 7-d-old seedlings were transferred to soil. Plants were grown in a growth chamber with the following conditions: long-day photoperiod (16 h of light/8 h of dark), light intensity of $170 \mu\text{mol m}^{-2} \text{s}^{-1}$, day/night temperatures of 21°C/17°C, and humidity of 65%. Shoot apices at bolting stage (before the opening of the first flower) were collected for ISH.

Sample Preparation for ISH

About 1 week after bolting, the shoot apex was dissected by removing the fully developed flowers. After fixation in FAA (3.7% [v/v] formaldehyde, 5% [v/v] acetic acid, and 50% [v/v] ethanol) overnight at 4°C, the samples were dehydrated and embedded in paraffin. Tissue blocks were then cut into 8- μm sections using a rotary microtome (Leica). The sections were processed by dewaxing, rehydration, and dehydration, as described previously (Yang et al., 2016).

RNA Probe Synthesis

For each gene, a cDNA fragment (800–1,000 bp) was amplified with gene-specific primers (Supplemental Table S1) and cloned into the pGEM-T Easy vector (Promega). After verification by sequencing, the plasmid was used as template for PCR with T7 and SP6 primers. The PCR products were then used as templates for in vitro transcription. According to the orientation of the cDNA insertion, either T7 or SP6 RNA polymerase was used to synthesize antisense RNA probes. These probes were labeled with Fluorescein-12-UTP or Digoxigenin-11-UTP (Roche). Note that probes can be stored at -20°C for several years.

Chromogenic ISH

Standard chromogenic ISH was performed as described previously (Yang et al., 2016). Briefly, the deparaffinized and dehydrated sections were hybridized with Digoxigenin-11-UTP-labeled probes and incubated at 55°C overnight. After hybridization, the probes were washed once with $2\times$ SSC and four times with $0.2\times$ SSC at 55°C. The slices were blocked in TBS-T buffer (50 mM Tris, pH 7.5, 0.9% [w/v] NaCl, and 0.3% [v/v] Triton X-100) plus 1% (w/v) Blocking Reagent (Roche) for 30 min and then incubated with anti-digoxigenin-AP

antibody (Roche; 1:1,000 dilution) for 2 h at room temperature. After washing with blocking buffer, samples were incubated in nitroblue tetrazolium/5-bromo-4-chloro-3-indolyl phosphate (Roche) color reaction buffer overnight at room temperature (22°C–23°C). For weakly expressed genes, the incubation time can be extended. The chromogenic signals were imaged using a Zeiss AxioImager M2 microscope fitted with a Zeiss Axiocam MRc color camera and a Plan Aplanachromat 20x/0.8NA objective.

RNA FISH

For FISH, sample preparation was similar to chromogenic ISH. After blocking, the sections were incubated with anti-fluorescein-POD antibody (Roche) for fluorescein-labeled probes and anti-digoxigenin-POD antibody (Roche) for digoxigenin-labeled probes. The hybridization was kept at room temperature for 3 h, and the signals were then detected using TSA Plus Fluorescein Fluorescence System (Perkin Elmer) or TSA Plus Cy5 Fluorescence System (Perkin Elmer). Images were taken with a Zeiss LSM700 confocal microscope equipped with a 20x/0.8NA dry objective. RNA FISH signals were detected in the LSM700 with a single 405/488/555/639 dichroic beam splitter. Laser excitation for fluorescein was 488 nm and detected with a band-pass filter BP 420-475 + BP 500-610. The Cy5 emission uses a long-pass LP 640 filter, and the wavelength range for detection was 640 to 700 nm.

Double RNA FISH

To check the mRNA coexpression of two genes, the sections were hybridized with two probes with different labels, one with digoxigenin and the other with fluorescein. After probe hybridization, the sections were first incubated with anti-fluorescein-POD antibody (1:200) for 2 h and detected with TSA Plus Fluorescein Fluorescence System. The samples were then treated with H_2O_2 (Sigma) to quench peroxidase activity of the first antibody (1 h of incubation in 1% [v/v] H_2O_2). The slices were further incubated with anti-digoxigenin-POD antibody (1:200) for 2 h and detected by TSA Plus Cy5 Fluorescence System (Perkin Elmer).

RNA FISH and Protein Immunofluorescence

To simultaneously detect mRNA and the corresponding protein, RNA FISH was first carried out as described above to reveal the RNA expression signals. After washing in PBS-T (phosphate-buffered saline containing 0.3% [v/v] Triton X-100) three times, 5 min each, the sections were kept in PBS-T Blocking Buffer (PBS containing 1% [w/v] BSA, 0.2% [w/v] powdered skim milk, and 0.3% [v/v] Triton X-100) for 30 min at room temperature. After blocking, samples were incubated with Alexa Fluor 488-conjugated GFP antibody (1:100 dilution; A-21311; Molecular Probes) overnight at 4°C. The excess antibody was washed in PBS-T three times, 5 min each, and fluorescence signal was observed with a Zeiss LSM700 confocal microscope.

Cell Wall and Nuclear Staining

For cell wall staining, sectioned samples were treated with 0.1% (w/v) Calcofluor White (Fluorescent Brightener 28; Sigma) for 5 min. After briefly washing in TBS-T two times, samples were imaged with a Zeiss LSM700 confocal microscope with 405 nm excitation and 425 to 475 nm emission.

For nuclear staining, $1 \mu\text{g mL}^{-1}$ DAPI (D9542; Sigma) was added to the samples shortly before observing the RNA FISH signals. Laser excitation was 405 nm for DAPI with a short-pass SP 555 filter. The wavelength range for detection was 400 to 555 nm.

Confocal Microscopy of Fluorescent Reporter Gene Expression

Shoot apices were dissected when the stem was ~ 1 cm in length. The meristem was placed in MS medium (Duchefa Biochemie; MS basal salt mixture) supplemented with vitamins ($100 \mu\text{g mL}^{-1}$ myo-inositol, $1 \mu\text{g mL}^{-1}$ nicotinic acid, $1 \mu\text{g mL}^{-1}$ pyridoxine hydrochloride, $1 \mu\text{g mL}^{-1}$ thiamine hydrochloride, and $2 \mu\text{g mL}^{-1}$ Gly) and 1% (w/v) Suc (Hamant et al., 2014). To label the cell boundaries, the samples were first stained with 0.1% (w/v) propidium iodide for 5 min and then imaged using Zeiss LSM700 with 20x/NA1.0 water-dipping objective or Leica SP8 with 25x/NA1.0 water-dipping

objective. The laser excitation settings were 488 nm for propidium iodide, GFP, or Venus. 3D rendering was performed using either Zen (Zeiss) or LAS X (Leica) software.

Detailed Protocols

Detailed step-by-step procedures for single and double RNA FISH and RNA FISH with protein immunolocalization are provided in Supplemental Protocol S1.

Accession Numbers

Sequence data from this article can be found in the GenBank/EMBL data libraries under the following accession numbers: NM_127349.4 (*WUS*), NM_001124926.2 (*CLV3*), NM_104916.4 (*STM*), NM_001345500.1 (*LFY*), NM_105581.3 (*API*), NM_001204009.1 (*AP2*), NM_115294.6 (*AP3*), NM_124774.3 (*CUC2*), NM_130082.4 (*FIL*), NM_125462.4 (*REV*), NM_001334957.1 (*AHP6*), NM_106017.4 (*PIN1*), NM_128434.4 (*HIS4*), NM_120697.3 (*CYCB1;2*), NM_001203049.1 (*MAD2*), NM_119481.3 (*CDC20*), NM_001203376.1 (*CCS52B*), NM_112849.5 (*BUB3*), and NM_128916.3 (*BUBR1*).

Supplemental Data

The following supplemental materials are available.

Supplemental Figure S1. Establishment of RNA FISH to investigate mRNA expression patterns in Arabidopsis shoot apices.

Supplemental Figure S2. Observation of cell wall and nucleus in meristem longitudinal sections by fluorescent dye staining.

Supplemental Figure S3. mRNA spatial distribution of meristem and flower development RNAs.

Supplemental Figure S4. Expression pattern of *AHP6* in the shoot apex and flower primordia.

Supplemental Figure S5. Expression patterns of cell cycle gene mRNAs.

Supplemental Figure S6. Expression patterns of MCC genes *MAD2*, *BUB3*, and *BUBR1*.

Supplemental Figure S7. *PIN1* expression patterns in the shoot apex.

Supplemental Figure S8. Expression patterns of auxin reporter *DR5::n3GFP* in the shoot apex.

Supplemental Table S1. Primers for in situ probes.

Supplemental Protocol S1. Single and double RNA FISH in Arabidopsis.

ACKNOWLEDGMENTS

We thank Jim Murray for sharing the *H4::DB-VENUS* seeds. We also thank Detlef Weigel for providing the Non-Radioactive in Situ Hybridisation with Arabidopsis Floral Tissue protocol.

Received August 8, 2019; accepted November 5, 2019; published November 13, 2019.

LITERATURE CITED

- Aida M, Ishida T, Fukaki H, Fujisawa H, Tasaka M (1997) Genes involved in organ separation in Arabidopsis: An analysis of the cup-shaped cotyledon mutant. *Plant Cell* **9**: 841–857
- Bartrina I, Otto E, Strnad M, Werner T, Schumling T (2011) Cytokinin regulates the activity of reproductive meristems, flower organ size, ovule formation, and thus seed yield in *Arabidopsis thaliana*. *Plant Cell* **23**: 69–80
- Bazin J, Baerenfaller K, Gosai SJ, Gregory BD, Crespi M, Bailey-Serres J (2017) Global analysis of ribosome-associated noncoding RNAs unveils new modes of translational regulation. *Proc Natl Acad Sci USA* **114**: E10018–E10027

- Benková E, Michniewicz M, Sauer M, Teichmann T, Seifertová D, Jürgens G, Friml J (2003) Local, efflux-dependent auxin gradients as a common module for plant organ formation. *Cell* **115**: 591–602
- Besnard F, Refahi Y, Morin V, Marteaux B, Brunoud G, Chambrier P, Rozier F, Mirabet V, Legrand J, Lainé S, et al (2014) Cytokinin signalling inhibitory fields provide robustness to phyllotaxis. *Nature* **505**: 417–421
- Blázquez MA, Soowal LN, Lee I, Weigel D (1997) *LEAFY* expression and flower initiation in *Arabidopsis*. *Development* **124**: 3835–3844
- Bleckmann A, Dresselhaus T (2016) Fluorescent whole-mount RNA *in situ* hybridization (F-WISH) in plant germ cells and the fertilized ovule. *Methods* **98**: 66–73
- Bowman JL, Alvarez J, Weigel D, Meyerowitz EM, Smyth DR (1993) Control of flower development in *Arabidopsis thaliana* by APETALA1 and interacting genes. *Development* **119**: 721–743
- Bowman JL, Smyth DR, Meyerowitz EM (1991) Genetic interactions among floral homeotic genes of *Arabidopsis*. *Development* **112**: 1–20
- Brand U, Fletcher JC, Hobe M, Meyerowitz EM, Simon R (2000) Dependence of stem cell fate in *Arabidopsis* on a feedback loop regulated by *CLV3* activity. *Science* **289**: 617–619
- Bruno L, Muto A, Spadafora ND, Iaria D, Chiappetta A, Van Lijsebettens M, Bitonti MB (2011) Multi-probe *in situ* hybridization to whole mount *Arabidopsis* seedlings. *Int J Dev Biol* **55**: 197–203
- Bruno L, Ronchini M, Gagliardi O, Corinti T, Chiappetta A, Gerola P, Bitonti MB (2015) Analysis of *AtGUS1* and *AtGUS2* in *Arabidopsis* root apex by a highly sensitive TSA-MISH method. *Int J Dev Biol* **59**: 221–228
- Carlsbecker A, Lee JY, Roberts CJ, Dettmer J, Lehesranta S, Zhou J, Lindgren O, Moreno-Risueno MA, Vatén A, Thitamadee S, et al (2010) Cell signalling by microRNA165/6 directs gene dose-dependent root cell fate. *Nature* **465**: 316–321
- Chitwood DH, Nogueira FTS, Howell MD, Montgomery TA, Carrington JC, Timmermans MC (2009) Pattern formation via small RNA mobility. *Genes Dev* **23**: 549–554
- Clark SE, Jacobsen SE, Levin JZ, Meyerowitz EM (1996) The *CLAVATA* and *SHOOT MERISTEMLESS* loci competitively regulate meristem activity in Arabidopsis. *Development* **122**: 1567–1575
- Denyer T, Ma X, Klesen S, Scacchi E, Nieselt K, Timmermans MCP (2019) Spatiotemporal developmental trajectories in the *Arabidopsis* root revealed using high-throughput single-cell RNA sequencing. *Dev Cell* **48**: 840–852.e5
- Fletcher JC, Brand U, Running MP, Simon R, Meyerowitz EM (1999) Signaling of cell fate decisions by *CLAVATA3* in *Arabidopsis* shoot meristems. *Science* **283**: 1911–1914
- Gälweiler L, Guan C, Müller A, Wisman E, Mendgen K, Yephremov A, Palme K (1998) Regulation of polar auxin transport by AtPIN1 in *Arabidopsis* vascular tissue. *Science* **282**: 2226–2230
- Hamant O, Das P, Burian A (2014) Time-lapse imaging of developing meristems using confocal laser scanning microscope. In V Žárský, and F Cvrčková, eds, *Plant Cell Morphogenesis*. Humana Press, Totowa, NJ, pp 111–119
- Heisler MG, Ohno C, Das P, Sieber P, Reddy GV, Long JA, Meyerowitz EM (2005) Patterns of auxin transport and gene expression during primordium development revealed by live imaging of the *Arabidopsis* inflorescence meristem. *Curr Biol* **15**: 1899–1911
- Himanen K, Woloszynska M, Boccardi TM, De Groeve S, Nelissen H, Bruno L, Vuylsteke M, Van Lijsebettens M (2012) Histone H2B monoubiquitination is required to reach maximal transcript levels of circadian clock genes in *Arabidopsis*. *Plant J* **72**: 249–260
- Izawa D, Pines J (2015) The mitotic checkpoint complex binds a second *CDC20* to inhibit active APC/C. *Nature* **517**: 631–634
- Jean-Baptiste K, McFaline-Figueroa JL, Alexandre CM, Dorrity MW, Saunders L, Bubb KL, Trapnell C, Fields S, Queitsch C, Cuperus JT (2019) Dynamics of gene expression in single root cells of *Arabidopsis thaliana*. *Plant Cell* **31**: 993–1011
- Jiang J (2019) Fluorescence *in situ* hybridization in plants: Recent developments and future applications. *Chromosome Res* **27**: 153–165
- Jiao WB, Schneeberger K (2017) The impact of third generation genomic technologies on plant genome assembly. *Curr Opin Plant Biol* **36**: 64–70
- Jiao Y, Meyerowitz EM (2010) Cell-type specific analysis of translating RNAs in developing flowers reveals new levels of control. *Mol Syst Biol* **6**: 419

- Jofuku KD, den Boer BG, Van Montagu M, Okamoto JK (1994) Control of *Arabidopsis* flower and seed development by the homeotic gene *APE-TALA2*. *Plant Cell* 6: 1211–1225
- Jones AR, Forero-Vargas M, Withers SP, Smith RS, Traas J, Dewitte W, Murray JAH (2017) Cell-size dependent progression of the cell cycle creates homeostasis and flexibility of plant cell size. *Nat Commun* 8: 15060
- Jönsson H, Heisler M, Reddy GV, Agrawal V, Gor V, Shapiro BE, Mjolsness E, Meyerowitz EM (2005) Modeling the organization of the *WUSCHEL* expression domain in the shoot apical meristem. *Bioinformatics* 21(Suppl 1): i232–i240
- Krizek BA, Meyerowitz EM (1996) Mapping the protein regions responsible for the functional specificities of the *Arabidopsis* MADS domain organ-identity proteins. *Proc Natl Acad Sci USA* 93: 4063–4070
- Lamb JC, Danilova T, Bauer MJ, Meyer JM, Holland JJ, Jensen MD, Birchler JA (2007) Single-gene detection and karyotyping using small-target fluorescence *in situ* hybridization on maize somatic chromosomes. *Genetics* 175: 1047–1058
- Levsky JM, Singer RH (2003) Fluorescence *in situ* hybridization: Past, present and future. *J Cell Sci* 116: 2833–2838
- Liao CY, Smet W, Brunoud G, Yoshida S, Vernoux T, Weijers D (2015) Reporters for sensitive and quantitative measurement of auxin response. *Nat Methods* 12: 207–210
- Long JA, Moan EI, Medford JL, Barton MK (1996) A member of the KNOTTED class of homeodomain proteins encoded by the *STM* gene of *Arabidopsis*. *Nature* 379: 66–69
- Mähönen AP, Bishopp A, Higuchi M, Nieminen KM, Kinoshita K, Törmäkangas K, Ikeda Y, Oka A, Kakimoto T, Helariutta Y (2006) Cytokinin signaling and its inhibitor AHP6 regulate cell fate during vascular development. *Science* 311: 94–98
- Mandel MA, Yanofsky MF (1995) A gene triggering flower formation in *Arabidopsis*. *Nature* 377: 522–524
- Mayer KF, Schoof H, Haecker A, Lenhard M, Jürgens G, Laux T (1998) Role of *WUSCHEL* in regulating stem cell fate in the *Arabidopsis* shoot meristem. *Cell* 95: 805–815
- Meyerowitz EM (1997) Genetic control of cell division patterns in developing plants. *Cell* 88: 299–308
- Michael TP, Jupe F, Bemm F, Motley ST, Sandoval JP, Lanz C, Loudet O, Weigel D, Ecker JR (2018) High contiguity *Arabidopsis thaliana* genome assembly with a single nanopore flow cell. *Nat Commun* 9: 541
- Otsuga D, DeGuzman B, Prigge MJ, Drews GN, Clark SE (2001) *REVOLUTA* regulates meristem initiation at lateral positions. *Plant J* 25: 223–236
- Prunet N, Yang W, Das P, Meyerowitz EM, Jack TP (2017) *SUPERMAN* prevents class B gene expression and promotes stem cell termination in the fourth whorl of *Arabidopsis thaliana* flowers. *Proc Natl Acad Sci USA* 114: 7166–7171
- Rhee SY, Birnbaum KD, Ehrhardt DW (2019) Towards building a plant cell atlas. *Trends Plant Sci* 24: 303–310
- Rogers KW, Schier AF (2011) Morphogen gradients: From generation to interpretation. *Annu Rev Cell Dev Biol* 27: 377–407
- Rozier F, Mirabet V, Vernoux T, Das P (2014) Analysis of 3D gene expression patterns in plants using whole-mount RNA *in situ* hybridization. *Nat Protoc* 9: 2464–2475
- Ryu KH, Huang L, Kang HM, Schiefelbein J (2019) Single-cell RNA sequencing resolves molecular relationships among individual plant cells. *Plant Physiol* 179: 1444–1456
- Sawa S, Watanabe K, Goto K, Liu YG, Shibata D, Kanaya E, Morita EH, Okada K (1999) *FILAMENTOUS FLOWER*, a meristem and organ identity gene of *Arabidopsis*, encodes a protein with a zinc finger and HMG-related domains. *Genes Dev* 13: 1079–1088
- Schmid M, Davison TS, Henz SR, Pape UJ, Demar M, Vingron M, Schölkopf B, Weigel D, Lohmann JU (2005) A gene expression map of *Arabidopsis thaliana* development. *Nat Genet* 37: 501–506
- Schoof H, Lenhard M, Haecker A, Mayer KF, Jürgens G, Laux T (2000) The stem cell population of *Arabidopsis* shoot meristems is maintained by a regulatory loop between the *CLAVATA* and *WUSCHEL* genes. *Cell* 100: 635–644
- Shargil D, Zemach H, Belausov E, Lachman O, Kamenetsky R, Dombrovsky A (2015) Development of a fluorescent *in situ* hybridization (FISH) technique for visualizing CGMMV in plant tissues. *J Virol Methods* 223: 55–60
- Shulse CN, Cole BJ, Ciobanu D, Lin J, Yoshinaga Y, Gouran M, Turco GM, Zhu Y, O'Malley RC, Brady SM, et al (2019) High-throughput single-cell transcriptome profiling of plant cell types. *Cell Rep* 27: 2241–2247.e4
- Skopelitis DS, Benkovics AH, Husbands AY, Timmermans MCP (2017) Boundary formation through a direct threshold-based readout of mobile small RNA gradients. *Dev Cell* 43: 265–273.e6
- Sorrell DA, Combettes B, Chaubet-Gigot N, Gigot C, Murray JA (1999) Distinct cyclin D genes show mitotic accumulation or constant levels of transcripts in tobacco bright yellow-2 cells. *Plant Physiol* 119: 343–352
- Stuart JM, Segal E, Koller D, Kim SK (2003) A gene-coexpression network for global discovery of conserved genetic modules. *Science* 302: 249–255
- Tirichine L, Andrey P, Biot E, Maurin Y, Gaudin V (2009) 3D fluorescent *in situ* hybridization using *Arabidopsis* leaf cryosections and isolated nuclei. *Plant Methods* 5: 11
- Urbanus SL, de Folter S, Shchennikova AV, Kaufmann K, Immink RG, Angenent GC (2009) In planta localisation patterns of MADS domain proteins during floral development in *Arabidopsis thaliana*. *BMC Plant Biol* 9: 5
- van de Corput MPC, Dirks RW, van Gijlswijk RPM, van de Rijke FM, Raap AK (1998) Fluorescence *in situ* hybridization using horseradish peroxidase-labeled oligodeoxynucleotides and tyramide signal amplification for sensitive DNA and mRNA detection. *Histochem Cell Biol* 110: 431–437
- Wang H, Chung PJ, Liu J, Jang IC, Kean MJ, Xu J, Chua NH (2014) Genome-wide identification of long noncoding natural antisense transcripts and their responses to light in *Arabidopsis*. *Genome Res* 24: 444–453
- Weigel D, Alvarez J, Smyth DR, Yanofsky MF, Meyerowitz EM (1992) *LEAFY* controls floral meristem identity in *Arabidopsis*. *Cell* 69: 843–859
- Woloszynska M, Le Gall S, Neyt P, Boccardi TM, Grasser M, Längst G, Aesaert S, Coussens G, Dhondt S, Van De Slijke E, et al (2019) Histone 2B monoubiquitination complex integrates transcript elongation with RNA processing at circadian clock and flowering regulators. *Proc Natl Acad Sci USA* 116: 8060–8069
- Xu XM, Wang J, Xuan Z, Goldshmidt A, Borrell PG, Hariharan N, Kim JY, Jackson D (2011) Chaperonins facilitate KNOTTED1 cell-to-cell trafficking and stem cell function. *Science* 333: 1141–1144
- Yadav RK, Perales M, Gruel J, Girke T, Jönsson H, Reddy GV (2011) *WUSCHEL* protein movement mediates stem cell homeostasis in the *Arabidopsis* shoot apex. *Genes Dev* 25: 2025–2030
- Yang W, Schuster C, Beahan CT, Charoensawan V, Peaucelle A, Bacic A, Doblin MS, Wightman R, Meyerowitz EM (2016) Regulation of meristem morphogenesis by cell wall synthases in *Arabidopsis*. *Curr Biol* 26: 1404–1415
- Yang W, Wightman R, Meyerowitz EM (2017) Cell cycle control by nuclear sequestration of *CDC20* and *CDH1* mRNA in plant stem cells. *Mol Cell* 68: 1108–1119.e3
- Yu H (2007) Cdc20: A WD40 activator for a cell cycle degradation machine. *Mol Cell* 27: 3–16
- Zhang TQ, Xu ZG, Shang GD, Wang JW (2019) A single-cell RNA sequencing profiles the developmental landscape of *Arabidopsis* root. *Mol Plant* 12: 648–660
- Zhu H, Hu F, Wang R, Zhou X, Sze SH, Liou LW, Barefoot A, Dickman M, Zhang X (2011) *Arabidopsis* Argonaute10 specifically sequesters miR166/165 to regulate shoot apical meristem development. *Cell* 145: 242–256